

GL03110 -149

DIPOLE-DIPOLE RESISTIVITY SURVEY OF A PORTION OF
THE COSO HOT SPRINGS KGRA
INYO COUNTY, CALIFORNIA

Richard C. Fox

EARTH SCIENCE LABORATORY
UNIVERSITY OF UTAH RESEARCH INSTITUTE
391-A Chipeta Way
Salt Lake City, Utah 84108

Date Published - May 1978

Prepared for the
DEPARTMENT OF ENERGY
DIVISION OF GEOTHERMAL ENERGY
UNDER CONTRACT EY-76-S-07-1601

NOTICE

This report was prepared to document work sponsored by the United States Government. Neither the United States nor its agent, the United States Department of Energy, nor any Federal employees, nor any of their contractors, subcontractors or their employees, makes any warranty, express or implied, or assumes any legal liability or responsibility for the accuracy, completeness, or usefulness of any information, apparatus, product or process disclosed, or represents that its use would not infringe privately owned rights.

NOTICE

Reference to a company or product name does not imply approval or recommendation of the product by the University of Utah Research Institute or the U.S. Department of Energy to the exclusion of others that may be suitable.

TABLE OF CONTENTS

	<u>Page</u>
ABSTRACT	1
INTRODUCTION	2
FIELD PROCEDURES	4
SURVEY RESULTS	6
Interpretation of Resistivity Pseudosections	6
Horizontal Resistivity Structure	13
SUMMARY AND CONCLUSIONS	18
ACKNOWLEDGEMENTS	19
REFERENCES	20
DISTRIBUTION LIST	

LIST OF ILLUSTRATIONS

		<u>Page</u>
Figure 1.	Location Map	3
Figure 2.	Electrode Geometry	5
Figure 3.	2-Dimensional computer model demonstrating effect of horizontal change in resistivity	7
Figure 4.	Apparent Resistivity Pseudosection Line 1	in pocket 1
Figure 5.	Apparent Resistivity Pseudosection Line 2 300 meter dipoles	in pocket 1
Figure 6.	Apparent Resistivity Pseudosection Line 2 150 meter dipoles	in pocket 1
Figure 7.	Apparent Resistivity Pseudosection Line 3	in pocket 1
Figure 8.	Apparent Resistivity Pseudosection Line 4	in pocket 1
Figure 9.	Apparent Resistivity Pseudosection Line 5	in pocket 1
Figure 10.	Apparent Resistivity Pseudosection Line 6	in pocket 1
Figure 11.	Apparent Resistivity Pseudosection Line 7	in pocket 1
Figure 12.	Apparent Resistivity Pseudosection Line 8	in pocket 1
Figure 13.	Apparent Resistivity Pseudosection Line 9	in pocket 1
Figure 14.	2-Dimensional Computer Model Line 1 Spread 2	in pocket 1
Figure 15.	2-Dimensional Computer Model Line 2 Spreads 2 and 3	in pocket 1
Figure 16.	2-Dimensional Computer Model Line 4	in pocket 1
Figure 17.	2-Dimensional Computer Model Line 5	in pocket 1
Plate I	Geologic Base Map	in pocket 2
Plate II	Generalized Near-Surface Resistivity Structure	in pocket 2

Plate III	Contour Map of First Separation (300 meter dipoles) and Third Separation (150 meter dipoles) Apparent Resistivity Values	in pocket 2
Plate IV	Generalized Resistivity Structure Approximately 300 Meters Below Surface	in pocket 2
Plate V	Contour Map of Third Separation Apparent Resistivity Values	in pocket 2
Plate VI	Contour Map of Sixth Separation Apparent Resistivity Values	in pocket 2

ABSTRACT

A detailed electrical resistivity survey of 54 line-km was completed at the Coso Hot Springs KGRA in September 1977. This survey has defined a bedrock resistivity low at least 4 sq mi (10 sq km) in extent associated with the geothermal system at Coso. The boundaries of this low are generally well defined to the north and west but not as well to the south where an approximate southern limit has been determined. The bedrock resistivity low merges with an observed resistivity low over gravel fill east of Coso Hot Springs.

A complex horizontal and vertical resistivity structure of the surveyed area has been defined which precludes the use of layered-earth or two-dimensional interpretive models for much of the surveyed area. In general the survey data indicate that a 10 to 20 ohm-meter zone extends from near surface to a depth greater than 750 meters within the geothermal system. This zone is bordered to the north and west by bedrock resistivities greater than 200 ohm-meters and to the south by bedrock resistivities greater than 50 ohm-meters. A combination of observed increases in: 1) fracture density (higher permeability), 2) alteration (high clay content), and 3) temperatures (higher dissolved solid content of ground water) within the bedrock low explain its presence.

INTRODUCTION

On behalf of the U. S. Department of Energy, Division of Geothermal Energy, a detailed surface geological and geophysical investigation of the Coso Hot Springs KGRA (Fig. 1) was undertaken by the Earth Science Laboratory, University of Utah Research Institute. The objectives of this work were 1) to collect data needed for detailed evaluation and interpretation of the results of the drilling of CGEH-1 (Galbraith, 1978), and 2) to help determine possible sites for future drill tests. Surface investigations included geologic and alteration mapping at a scale of 1:24,000 (Hulen, 1978), a low-altitude aeromagnetic survey (Fox, 1978), and an inline dipole-dipole resistivity survey. This report describes only the results of the resistivity survey.

Earlier studies of the electrical properties of rocks within the Coso area were made by Furgerson (1973) and by Jackson and others (1977). Furgerson's studies consisted of Schlumberger resistivity soundings and roving-dipole resistivity mapping. Jackson's work included Schlumberger resistivity soundings, audio-magnetotelluric (AMT) resistivity soundings, and telluric resistivity mapping. Both studies, by design, were reconnaissance in nature. In contrast, the present work was done to map horizontal and vertical resistivity structure in detail in an attempt to determine possible correlation with the geothermal system and to help delineate the extent of the geothermal system.



FIELD PROCEDURES

The field survey was performed under contract by Mining Geophysical Surveys of Tucson, Arizona. An inline, dipole-dipole electrode geometry was used (Fig. 2). The survey provides resolution both of horizontal and of vertical resistivity contrasts because the field procedure generates both horizontal profiling and vertical sounding measurements. Measurements were made at dipole separations, $n \times a$, of $n = 0.5, 1, 2, 3, 4, 5$ and 6 , where a equals the dipole length. A grid of three north-south lines and six east-west lines was surveyed to map the resistivity structure of a 41 sq km (16 sq mi) area. A total of 54 line-km of line was surveyed in 20 field days, 40.8 line-km using $a = 300$ m dipoles and 13.2 line-km using $a = 150$ m dipoles (see Plate II).

Measurements were made in the time-domain mode. Instrumentation consisted of a Data Control Systems model IPR-2 receiver (Newmont-type) and a Geotronics model FT-20A transmitter. The signal-to-noise ratio generally was good even for signals below 1 mv. Repeat measurements were made by interchanging current and potential dipoles to determine the accuracy of measurements. These repeat measurements are shown on the data pseudosections in Figures 4-13. Percentage differences were calculated for each of 121 repeat measurements: the mean and standard deviations are 8.2% and 8.8% respectively. In view of the wide range of observed resistivity values and of past experience with resistivity surveys, this amount of error is quite reasonable.

ELECTRODE GEOMETRY

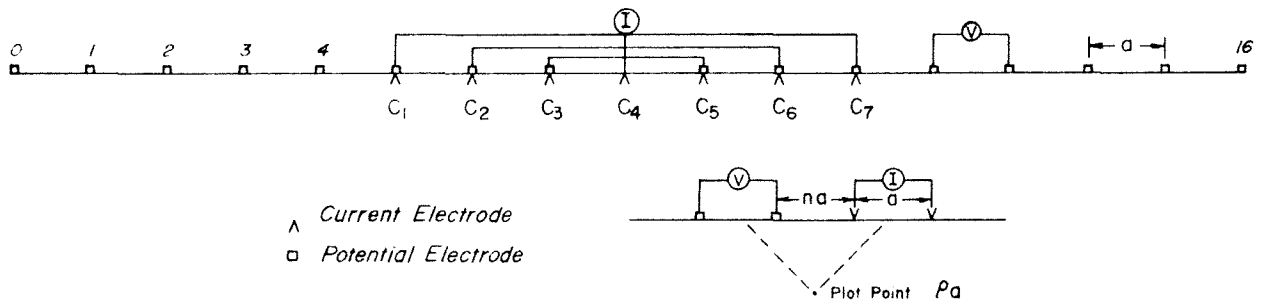


FIGURE 2

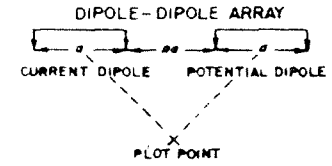
SURVEY RESULTS

Interpretation of Resistivity Pseudosections

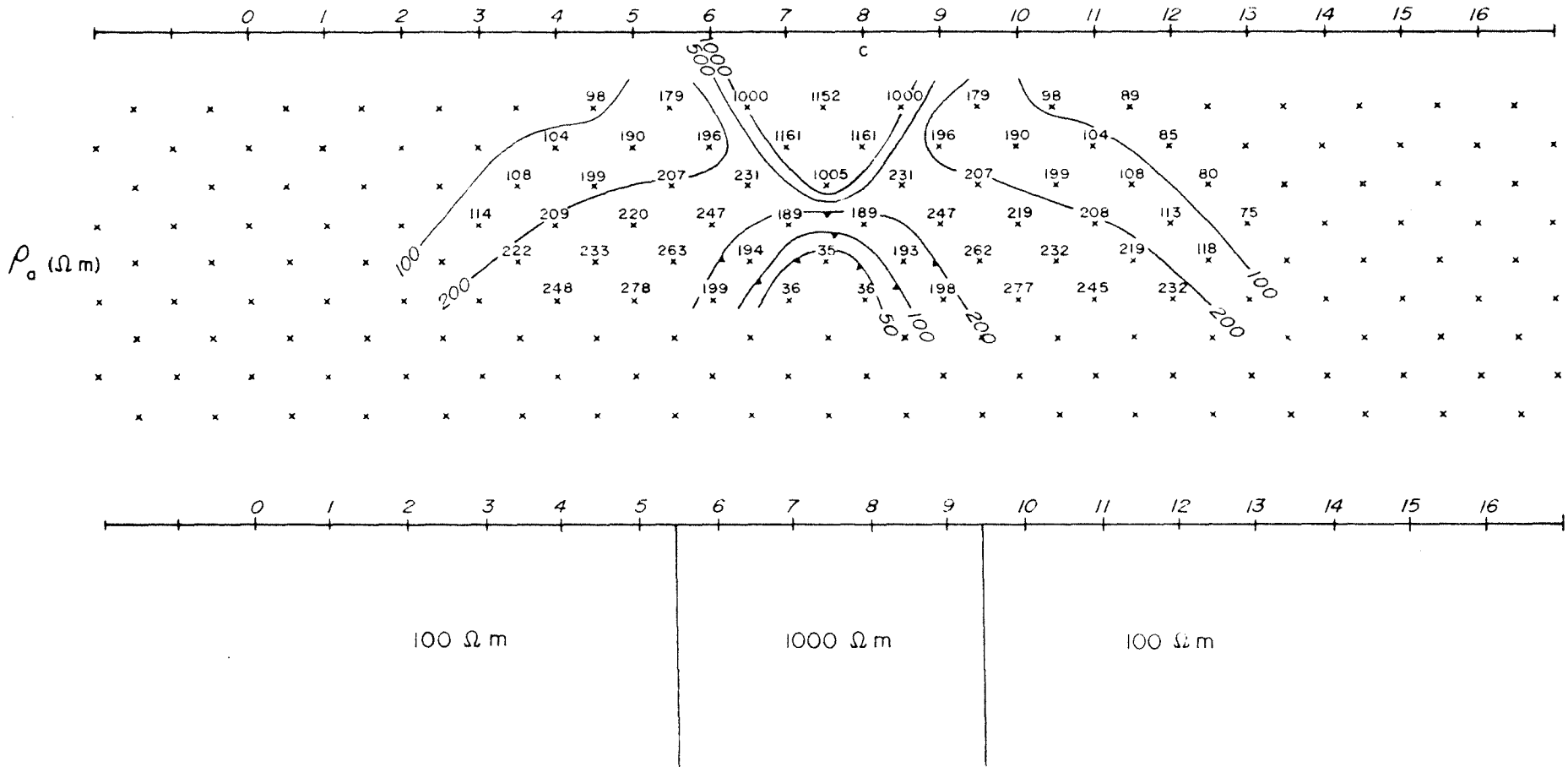
Line 1 (300 m dipoles, Fig. 4) is an east-west resistivity cross section 9.6 km in length extending from a point west of Sugarloaf Mountain to a point east of Coso Hot Springs (see Plate II for line locations). West of Sta. 13 apparent resistivities are high at short electrode separations, presumably showing volcanic rocks overlying 50 to 100 ohm-meter basement rock. Low apparent-resistivity values at greater electrode separations in this area are less than true (intrinsic) resistivity values partly because of the extreme resistivity contrast between the volcanic rocks and the basement rocks (see Fig. 3) and because of the effect of horizontal changes in resistivity along the line. Low apparent resistivity probably associated with the geothermal system extends from Sta. 13 to Sta. 25, a distance of 3.6 km. Resistivity values less than 10 ohm-meters in this interval are interpreted to be an effect of a fault zone subparallel to the Line as shown on the geologic map of Plate I. East of Sta. 25 the 10 ohm-meter and lower values are related to gravel fill. The lack of an increase in apparent resistivity with depth indicates that the thickness of the conductive gravel layer is greater than 500 m, assuming a resistivity contrast exists between the gravel and underlying bedrock.

A two-dimensional computer model of this line from Sta. 8 to Sta. 24 (Fig. 14) shows the interpreted resistivity structure. A two-dimensional model is a valid assumption if resistivity features extend at nearly right angles from the line for a distance of 3 dipoles to either side of the line

DIPOLE - DIPOLE ARRAY
 APPARENT RESISTIVITY



$a = \text{---} x \text{---}$ meters



2-DIMENSIONAL MODEL DEMONSTRATING REVERSAL IN
 APPARENT RESISTIVITY AT DEPTH WITH INCREASING DIPOLE SEPARATION
 DUE TO A HORIZONTAL CHANGE IN RESISTIVITY

(G. W. Hohmann, personal communication). The computed resistivity values are in general agreement with the observed values indicating a reasonable interpretation of the resistivity structure. Points of difference between computed and observed values are partly the result of non-two-dimensional structure along the line such as the subparallel fault zone. The western end of this model approximates the resistivity structure between Sugarloaf Mountain and the three rhyolite domes immediately to the north (see Plate II for line location). A geologic section through this area would probably show a rhyolite neck extending to depth below the 3000 ohm-meter rhyolite layer. While this section would be geologically more accurate the indicated resistivity structure is more accurate with respect to current flow. Since the necks of the rhyolite domes are three-dimensional, i.e., inverted cones or funnel shaped, and more resistive than their host rock the electrical current actually flows around rather than through them. Since a two-dimensional computer model is not limited in strike length a resistive zone that represents a neck would appear as a resistive dike through which current would be forced to flow. A three-dimensional model that limited the strike length of the resistive zone would be more accurate both geophysically and geologically.

Line 2 (300 m dipoles, Fig. 5) is a north-south resistivity cross section 9.6 km in length. Low resistivities apparently related to the geothermal system extend from Sta. 9 to Sta. 23, a distance of 4.2 km. North of Sta. 23 resistivity increases rapidly while south of Sta. 9 the resistivity begins to increase more slowly, and the low resistivity anomaly cannot be said to be cut off although AMT measurements taken at 7.5 Hz in this area show apparent

resistivities greater than 50 ohm-meters at the southern end of Line 2 (Jackson; personal communication).

The interpreted resistivity structure between Sta. 8 and Sta. 32 was determined by two-dimensional computer modeling (Fig. 15). A comparison of computed and observed values indicates a reasonable interpretation. The plus 20 ohm-meter values at depth in the Sta. 14 to Sta. 17 interval is another example of the effect of horizontal resistivity changes. In this instance an increase in apparent resistivity with increasing dipole separation was generated as the transmitting and receiving dipoles were moved from low to higher resistivity zones. The two 15 ohm-meter zones, Sta. 9 to Sta. 10 and Sta. 13 to Sta. 14, extending to depth, are interpreted to be fault zones. An interesting and important feature is the apparent resistivity low which approaches the surface in the Sta. 12 to Sta. 14 interval. This low is immediately adjacent to the Devil's Kitchen surface fumarole activity and is likely due to hot fluids and open fractures associated with this activity.

Line 2 (150-m dipoles, Fig. 6) was run to add detail to the resistivity structure observed on the 300-m dipole line. The data essentially represent a closer look at the upper three separations of the 300-m dipole data and present a more accurate picture of the complex near-surface resistivity structure. Near-surface apparent resistivity is mainly high, with marked decrease at depth. Interpreted depth to lower resistivity rock averages 90 m. The interval 12.5 to 13.5 shows low near-surface resistivity again corresponding with the Devil's Kitchen area.

Line 3 is an east-west resistivity profile across the CGEH-1 drill-site.

The resistivity structure on this line is similar to that observed on Line 1. Observed resistivity values less than 20 ohm-meters between Sta. 7 and Sta. 12 are related to the geothermal system and to a major north-northeast-trending fault zone defined by Lines 4 and 6 to the north. A plus 30 ohm-meter zone extends to depth between Sta. 12 and Sta. 16. Low resistivity values east of Sta. 17 are related to geothermal activity along the Coso Hot Springs fault zone and to gravel fill interpreted to be thicker than 500 m at the extreme eastern end of the line.

Line 4 was run across an apparent north-northeast-trending fault zone noted by shearing in outcrop. A two-dimensional computer model (Fig. 16) shows the interpretation of the resistivity structure observed on this line. The 450 m wide, 20 ohm-meter zone extending to depth between Sta. 7 and Sta. 10 is interpreted to be an expression of the fault zone in crystalline basement rock. This fault zone is one of the major north-northeast-trending structures observed in the area (see Plate I).

Line 5 is an east-west resistivity section with characteristics similar to the Sta. 8 to Sta. 24 interval on Line 1. A two-dimensional computer model of the line is shown as Fig. 17. The 10 ohm-meter zone shown on this model represents the geothermal system near its southern edge.

Line 6 was run to determine if the fault zone mapped on Line 4 extends to the south towards CGEH-1. The near-surface, low resistivity zone between Sta. 8 and Sta. 9 is interpreted to be the southern extension of this structure.

Line 7 was run west of the rhyolite domes to test for possible low resistivity, west-northwest-trending fault zones, and to determine the resistivity structure associated with the fumarole at the southwestern end of Sugarloaf Mountain. Near-surface, high resistivity values between Sta. 3 and Sta. 8 are associated with subsurface volcanics while the low resistivity zone at depth in this interval of less than 20 ohm-meters is caused in part by horizontal decreases in resistivity outside this interval. In particular the Sta. 1 to Sta. 3 interval shows a zone of low resistivity, less than 20 ohm-meters, associated with the fumarole. This low-resistivity zone probably extends from the surface to depth. If a conductive fault zone is associated with this fumarole, its strike has not been established.

A near-surface, high-resistivity layer of plus 100 ohm-meters material thickens to the north from Sta. 8 to the northern end of the line and is associated with crystalline basement rock. Resistivity values less than 100 ohm-meters at depth in this interval probably reflect an increase in water content of the basement rocks below the water table.

Line 8 is a 150-m dipole line run along the eastern edge of Devil's Kitchen. Apparent resistivity values greater than 100 ohm-meters reflect varying thicknesses of overlying volcanic material. At Sta. 11 the high resistivity rhyolite zone probably extends to depth. The 8 ohm-meter anomaly below this station, at n=6, is another example of a resistivity reversal due to horizontal changes in resistivity as shown on Figure 3. The near-surface zone of less than 20 ohm-meters below Sta. 16 is related to the altered rock at Devil's Kitchen while the somewhat higher resistivities at depth indicate

that the alteration is limited to the near-surface. Donald White, of the USGS (personal communication) has noted that the alteration at Devil's Kitchen is a near-surface process involving oxidation of H_2S vapors producing H_2SO_4 when mixed with ground water which attacks the surrounding rocks. This chemical model is clearly supported by the observed resistivity pattern. The 9 ohm-meter anomaly in the Sta. 20 to Sta. 21 interval is associated with the fault zone that lies subparallel to Line 1 and the 6 ohm-meter anomaly to the north is probably related to a parallel structure. A comparison of this line with the 150 m dipole Line 2 (Fig. 6) shows that they are similar, indicating at least 600 m of east-west structural continuity between these lines. The obvious east-west structural control of the less than 10 ohm-meter anomalies on line 8 explains the lack of good correlation between the computed and the observed resistivity values on Line 1 (Figs. 4 and 14). As a result, a north-trending, two-dimensional, 10 ohm-meter near-surface zone is not a valid model for the Sta. 16 to Sta. 20 E interval on Line 1.

Line 9 is a 150 m dipole line run along the southern edge of Devil's Kitchen. The pervasive 30 to 50 ohm-meter values are somewhat surprising as lower values, comparable to those observed on Line 8 and associated with alteration, were expected. The higher values suggest that the alteration exposed at the southern edge of Devil's Kitchen is also the southern limit of alteration which is apparently limited to the immediate area of H_2S gas emanation. This observation is again consistent with White's model of the alteration process. The 30-50 ohm-meter zone is related to the topographically subdued rhyolite dome at the southern edge of the Devil's Kitchen and represents an area of relatively higher resistivity, which extends

to depth, within the overall bedrock resistivity low. A resistivity contrast is observed at Sta. 13 which corresponds to a mapped fault. The lower resistivities to the east are related to basement rock and indicate a continuation of the bedrock resistivity low in this area.

Horizontal Resistivity Structure

The horizontal resistivity structure of the surveyed area is discussed with reference to the data shown in plan view on Plates II through VI. These Plates are overlays to the geologic base map, Plate I.

Plate II shows the interpreted near-surface resistivity distribution. Locations of resistivity contacts and intrinsic resistivity values were taken directly from two-dimensional computer models for Lines 1 through 5 and were interpreted by inspection for the other lines. Catalogs of theoretical resistivity models show that the diagonal contour patterns are associated with near vertical resistivity contrasts and this association was used to interpret Lines 6 through 9. The region of 1,000-7,000 ohm-meters resistivity in the western portion of the survey coincides with outcrop of rhyolite domes. Resistivity values over crystalline basement outcrop range from 10 ohm-meters, just west of Coso Hot Springs and just east of Devil's Kitchen, to over 500 ohm-meters in the northern and northwestern parts of the area. Basement resistivity values generally decrease to the south and east.

Plate III is a contour map of first separation, $n=1$, apparent resistivity values. Almost all of the surface geothermal manifestations in the Coso area occur within the 20 ohm-meter contour line. Of particular interest is the narrow zone of less than 10 ohm-meters parallel to Line 1 at the center of the

map. Detailed geologic mapping indicates that this zone corresponds with a major east-northeast-trending fault zone (Plate I). The strong similarity between the interpreted resistivity, Plate II, and the apparent resistivity, Plate III, indicates the limited effect of lateral resistivity averaging at $n=1$.

Plate IV shows the interpreted true resistivity structure at an approximate depth of 300 meters. This interpretation is supported by two-dimensional computer modeling of individual lines, where a two-dimensional approximation is reasonable, and by inference from catalogs of two-dimensional resistivity models (Ludwig, 1967) and three-dimensional models (Hohmann, 1975). The 1000-7000 ohm-meter zone is the inferred root system of the rhyolite domes. Resistivities shown on this Plate are generally lower relative to those shown in Plate II and reflect the increase in pore fluid below the water table. Depth to the water table is probably 50 to 100 m within the surveyed area. The western edge of the 10-20 ohm-meter zone parallel to Line 2 is generally well established by modeling while the eastern edge of this zone is poorly defined. Recent geologic mapping and the geologic log of CGEH #1 suggest the western edge of this zone may be related to a contact between a Cretaceous (?) leuco-granite intrusive to the east and older metamorphic rock to the west (Hulen 1978). The 30-50 ohm-meter circular feature is related to the rhyolite dome just south of Devil's Kitchen. The narrow, 10 ohm-meter zone subparallel to Line 1 is the expression of the major ENE trending fault zone referred to on Plate III. The 10-20 ohm-meter zone on Line 7 is spatially related to a fumarole on the southwestern end of Sugarloaf Mountain. If linear, the eastern and western limits of this low resistivity

feature have not been determined.

Computed models of Lines 1, 2 and 5 (Figs. 14, 15 and 17) show 20 ohm-meter resistivity values within the geothermal system for the depth range 300 to 1000 m. Increasing the intrinsic resistivity values of the computer models from 20 to 50 ohm-meters, below 300 m generates higher apparent-resistivity values than those observed at the greater dipole separations. The Induction Electrolog of CGEH #1 shows resistivity values gradually increasing from 10 ohm-meters to 50 ohm-meters for the 300 to 1000 m depth interval. If the resistivity log of CGEH-1 is taken as representative of the resistivity structure at depth within the geothermal system, then it appears that 50 ohm-meters is the upper limit of intrinsic resistivity for the system to a 1000 m depth. This conclusion is consistent with the model results where a gradual increase in resistivity to 50 ohm-meters at a depth of 1000 m is permissible.

Plate V shows the contoured apparent resistivity values observed at a dipole separation of $n=3$. The apparent-resistivity structure shown on this plate is less complex than the interpreted resistivity structure of Plate IV at a comparable depth. At the third separation, vertical and lateral resistivity values are averaged over a larger volume of rock which results in gradational changes in the apparent resistivity values. The resistivity low defined by the 20 ohm-meter contour line covers a 4 sq mi (10 sq km) area and is open to the east and southeast. To the east the bedrock low merges with low resistivity values of the gravel-filled basin east of Coso Hot Springs. The extent of the bedrock low to the southeast is not delineated by this

survey. Although not fully defined by the results of this survey, the inferred southern limit of the low is supported by the results of AMT soundings in this area (D. B. Jackson, personal communication). The unsurveyed bedrock area is 2 to 3 sq mi (2-5 sq km) in extent.

In the absence of any obvious change in rock type, this bedrock resistivity low is probably caused by a combination of observed increases in: 1) fracture density (higher permeability), 2) hydrothermal alteration (higher clay content) and/or, 3) temperature (higher dissolved solid content). The results of recent detailed geologic mapping by Hulen (1978) and shallow temperature measurements by LaSchack (1977) support this conclusion. The significance of this interpretation should be judged in light of the results of recent work by Moskowitz and Norton (1977) which has shown that low resistivities associated with geothermal anomalies are "a complex function of fluid circulation patterns, fluid composition, and the distribution of conductive minerals produced by the reaction between circulating fluids and rocks." They point out that in many cases low near-surface resistivity anomalies cannot be entirely accounted for by hot circulating saline fluids and that observations of high thermal gradients associated with low-resistivity anomalies are not unique indications of a high-energy geothermal resource at shallow crustal depths.

Plate VI a contour map of sixth separation, $n=6$, apparent resistivity values demonstrates the effects of lateral changes in resistivity. Overlaying this map on the map of first separation values, Plate III, shows that the position of resistivity highs and lows are generally reversed. The low, less

than 20 ohm-meters on Plate VI, west of line 2, is produced by the extreme contrast in resistivity between the rhyolite and host rock. The transmitting and receiving dipoles for sixth-separation measurements were 1.8 km apart and located in relatively lower resistivity host rock which causes this apparent low at depth. The plus 20 ohm-meter values observed in the center of Plate VI, near Devil's Kitchen, were caused by the reverse situation where the transmitting and receiving dipoles were located in relatively higher resistivity zones. Referring again to Figure 3, this reversal in apparent resistivity with increasing dipole separation is shown to be mainly the result of horizontal changes in resistivity rather than vertical.

SUMMARY AND CONCLUSIONS

This survey has defined a bedrock resistivity low at least 4 sq mi (10 sq mi) and up to 6 sq mi (15.5 sq km) in extent associated with the geothermal system at Coso. The boundaries of this low are generally well defined to the north and west by 5- to 10-fold increases in resistivity compared to resistivities observed within the low. The extent of the anomaly is not as well defined to the south but resistivity values generally increase in this direction and the approximate southern limit has been determined. The bedrock resistivity low merges with an observed resistivity low over gravel fill east of Coso Hot Springs.

A complex horizontal and vertical resistivity structure of the surveyed area has been defined which precludes the use of layered-earth or two-dimensional interpretive models for much of the surveyed area. In general the survey data indicate that a 10 to 20 ohm-meter zone extends from near surface to a depth greater than 750 meters within the geothermal system. A combination of observed increases in: 1) fracture density (higher permeability), 2) alteration (high clay content), (Hulen, 1978) and 3) temperatures (higher dissolved solid content of ground water) within the bedrock low explain its presence.

Additional resistivity work would be necessary to fully define the extent of the bedrock low to the southeast. Detailed lines, using 150-m dipoles, would help to further delineate major north-northeast and west-northwest structural features within the low.

ACKNOWLEDGEMENTS

This work was funded by the Department of Energy, Division of Geothermal Energy contract EY-76-S-07-1601. Related Coso studies are being continued under Department of Energy, Division of Geothermal Energy contract EG-78-C-07-1701. The author thanks William F. Isherwood of the United States Geological Survey for his review of and comments on this report.

REFERENCES CITED

- Fox, R. C., 1978, "Low-Altitude Aeromagnetic Survey of a Portion of the Coso Hot Springs KGRA, Inyo County, California," UURI-ES1 Report, DOE Contract EY-76-S-07-1601.
- Furgerson, R. B., 1973, Progress Report on Electrical Resistivity Studies, Coso Geothermal Area, Inyo County, California, NWC Technical Publication S 497, Propulsion Development Dept., China Lake, California.
- Hohmann, G. W., 1975, "Three-Dimensional Induced Polarization and Electromagnetic Modeling", Geophysics, Vol. 40, No. 2, pp. 309-324.
- Hulen, J. B., 1978, Geology and Alteration of the Coso Geothermal Area, Inyo County, California, UURI-ESL Report, DOE Contract EG-78-C-07-1701.
- Jackson, D. B., O'Donnell, J. E., and Gregory, D. I., 1977, "Schlumberger Soundings, Audio-Magnetotelluric Soundings, and Telluric Mapping in and Around the Coso Range, California," USGS, Open File Report, pp. 77-120.
- LeSchack, L. A., Lewis, J. E., and Chang, D. C., 1977, Rapid reconnaissance of geothermal prospects using shallow temperature surveys: Semi-Annual Technical Report, Development and Resources Transportation Co.; DOE Contract EG-77-C-01-4-21.
- Ludwig, C. S., 1967, Theoretical Induced Polarization and Resistivity Response from the Dual Frequency System, Collinear Dipole-Dipole Array, " Vol. 1 and 2, Heinrichs Geoexploration Company.

Moskowitz, B. and Norton, D., 1977, A Preliminary Analysis of Intrinsic Fluid and Rock Resistivity in Active Hydrothermal Systems: J. of Geophysical Research, v. 82, no. 36.

FIGURE CAPTIONS

- Figure 4 Apparent Resistivity Pseudosection Line 1
- Figure 5 Apparent Resistivity Pseudosection Line 2, 300 meter dipoles
- Figure 6 Apparent Resistivity Pseudosection Line 2, 150 meter dipoles
- Figure 7 Apparent Resistivity Pseudosection Line 3
- Figure 8 Apparent Resistivity Pseudosection Line 4
- Figure 9 Apparent Resistivity Pseudosection Line 5
- Figure 10 Apparent Resistivity Pseudosection Line 6
- Figure 11 Apparent Resistivity Pseudosection Line 7
- Figure 12 Apparent Resistivity Pseudosection Line 8
- Figure 13 Apparent Resistivity Pseudosection Line 9
- Figure 14 2-Dimensional Computer Model Line 1, Spread 2
- Figure 15 2-Dimensional Computer Model Line 2, Spread 2 and 3
- Figure 16 2-Dimensional Computer Model Line 4
- Figure 17 2-Dimensional Computer Model Line 5

DISTRIBUTION LIST

External

David N. Anderson	Geothermal Resources Council, Davis, CA.
R.J. Andrews	Rocky Mountain Well Log Services, Denver, CO.
James K. Applegate	Boise State University, Boise, ID.
Sam Arentz, Jr.	Steam Corporation of America, Salt Lake City, UT.
Carl F. Austin	Geothermal Technology, NWC, China Lake, CA.
Lawrence Axtell	Geothermal Services, Inc., San Diego, CA.
Charles Bacon	USGS, Menlo Park, CA.
C. Forest Bacon	California Division of Mines & Geology, Sacramento, CA.
Larry Ball	DOE/DGE, Washington, DC.
Ronald Barr	Earth Power Corporation, Tulsa, OK.
H.C. Bemis	Fluid Energy Corporation, Denver, CO.
David D. Blackwell	Southern Methodist University, Dallas, TX.
Gunnar Bodvarsson	Oregon State University, Corvallis, OR.
C.M. Bonar	Atlantic Richfield Co., Dallas, TX.
David Boore	Stanford University, Stanford, CA.
Roger L. Bowers	Hunt Energy Corporation, Dallas, TX.
Jim Bresee	DOE/DGE, Washington, DC.
A.J. Brinker	Al-Aquitaine Exploration, Ltd., Denver, CO.
William D. Brumbaugh	Conoco, Ponca City, OK.
Larry Burdge	EG&G Idaho, Idaho Falls, ID.
Scott W. Butters	Terra Tek, Salt Lake City, UT.
Glen Campbell	Gulf Min. Resource Company, Denver, CO.
Bob Christiansen	USGS, Menlo Park, CA.
Eugene V. Ciancanelli	Consulting Geologist, San Diego, CA.
Jim Combs	Geothermal Services, Inc., San Diego, CA.
F. Dale Corman	O'Brien Resources, Inc., Kentfield, CA.
Ritchie Coryell	National Science Foundation, Washington, DC.
R. Corwin	University of California, Berkeley, CA.
James Cotter	DOE/NV, Las Vegas, NV.
Gary Crosby	Phillips Petroleum Company, Del Mar, CA.
K.R. Davis	Thermal Power Company, San Francisco, CA.
Jere Denton	Southland Royalty Company, Fort Worth, TX.
William Dolan	Amax Exploration Inc., Denver, CO.
Earth Sciences Division Library	Lawrence Berkeley Laboratory, Berkeley, CA.
Robert C. Edmiston	Chevron Resources Company, San Francisco, CA.
Wilf Elders	University of California, Riverside, CA.
Samuel M. Eisenstat	Geothermal Exploration Company, New York, NY.
M.C. Erskine, Jr.	Eureka Resource Associates, Berkeley, CA.
Domenic J. Falcone	Geothermal Resources International, Marina del Rey, CA.
Glen Faulkner	USGS, Water Resources Division, Menlo Park, CA.
Val A. Finlayson	Utah Power and Light Company, Salt Lake City, UT.
Joseph N. Fiore	DOE/NV, Las Vegas, NV.
Robert T. Forest	Phillips Petroleum Company, Reno, NV.

Robert O. Fournier	USGS, Menlo Park, CA.
Frank Frischknecht	U.S. Geological Survey, Denver, CO.
Gary Galyardt	U.S. Geological Survey, Denver, CO.
N.E. Goldstein	Lawrence Berkeley Laboratory, Berkeley, CA.
Steven M. Goldstein	The Mitre Corporation, McLean, VA.
Bob Greider	Intercontinental Energy Co., Denver, CO.
John Griffith	DOE/ID, Idaho Falls, ID.
J.H. Hafenbrack	Exxon Co. USA, Denver, CO.
W.R. Hahman	Arizona Bureau of Geology & Mineral Technology Tucson, AZ.
Dee C. Hansen	Utah State Engineer, Salt Lake City, UT.
V. Nobel Harbinson	O'Brien Resources, Incorporated, Toronto, Ontario, Canada.
Norman Harthill	Group Seven, Incorporated, Golden, CO.
Margaret E. Hinkle	USGS-Exploration Research, Golden, CO.
John V. Howard	Lawrence Berkeley Laboratory, Berkeley, CA.
Don Hull	Oregon Dept. of Geology & Mineral Industries, Portland, OR.
Gerald W. Hutterer	Intercontinental Energy Corporation, Englewood, CO.
William F. Isherwood	USGS, Menlo Park, CA.
Dallas Jackson	USGS, Hilo, HI.
Jimmy J. Jacobson	Battelle Pacific Northwest Labs., Richland, WA.
Laurence P. James	Denver, CO.
George R. Jiracek	University of New Mexico, Albuquerque, NM.
Richard L. Jodry	Richardson, TX
Max Jones	Sierra Pacific Power, Reno, NV.
Lewis J. Katz	Utah Geophysical, Incorporated, Salt Lake City, UT.
Paul Kasameyer	Lawrence Livermore Laboratory, Livermore, CA.
George Keller	Colorado School of Mines, Golden, CO.
Paul Kintzinger	Los Alamos Scientific Laboratory, Jemez Springs, NM.
John W. Knox	Sunoco Energy Development Company, Dallas, TX.
James B. Koenig	Geothermex, Berkeley, CA.
Robert P. Koeppen	Oregon Institute Technology, Klamath Falls, OR.
Frank C. Kresse	Harding-Lawson Associates, San Rafael, CA.
Mark Landisman	University of Texas, Dallas, Richardson, TX.
Art Lange	AMAX Exploration, Incorporated, Denver, CO.
A.W. Laughlin	Los Alamos Scientific Laboratory, Los Alamos, NM.
Guy W. Leach	Oil Development Company of Texas, Amarillo, TX.
R.C. Lenzer	Phillips Petroleum Company, Del Mar, CA.
Paul Lienau	OIT, Klamath Falls, OR.
Mark A. Liggett	Cyprus Georesearch Company, Los Angeles, CA.
James O. McClellan	Geothermal Electric Systems Corporation, Salt Lake City, UT.
Robert B. McEuen	Woodward Clyde Consultants, San Francisco, CA.
Don C. McMillan	Utah Geological & Mineral Survey, Salt Lake City, UT.

J.R. McNitt	Energy and Mineral Development Branch, United Nations, NY.
Don R. Mabey	USGS, Denver, CO.
Skip Matlick	Republic Geothermal, Santa Fe Springs, CA.
Tsvi Meidav	Consultant, Berkeley, CA.
Frank G. Metcalfe	Geothermal Power Corporation, Novato, CA.
John Mitchell	Idaho Dept. of Water Resources, Boise, ID.
Frank Morrison	University of California, Berkeley, CA.
L.J. Patrick Muffler	USGS, Menlo Park, CA.
Clayton Nichols	DOE/DGE, Washington, DC.
H.E. Nissen	Aminoil USA, Houston, TX.
Denis Norton	University of Arizona, Tucson, AZ.
Franklin Olmsted	USGS, Menlo Park, CA.
Carel Otte	Union Oil Company, Los Angeles, CA.
Richard H. Pearl	Colorado Geological Survey, Denver, CO.
Wayne Peeples	Southern Methodist University, Dallas, TX.
B.J. Perry	Mono Power Company, Rosemead, CA.
Harvey S. Price	Intercomp Resource Development & Engineering Inc. Houston, TX.
Alan O. Ramo	Sunoco Energy Development Company, Dallas, TX.
Robert W. Rex	Republic Geothermal, Inc., Santa Fe Springs, CA.
Barbara Ritzma	Science & Engineering Department, University of Utah, Salt Lake City, UT.
Jack Salisbury	DOE/DGE, Washington, DC.
Robert San Martin	New Mexico Energy Institute, Las Cruces, NM.
Konosuke Sato	Metal Mining Agency of Japan, Minato-Ku, Tokyo.
Robert Schultz	EG&G Idaho, Idaho Falls, ID.
John V.A. Sharp	Hydrosearch, Inc., Reno, NV.
Wayne Shaw	Getty Oil Company, Bakersfield, CA.
Gregory L. Simay	City of Burbank, Public Service Dept., Burbank, CA.
W.P. Sims	DeGolyer and MacNaughton, Dallas, TX.
H.W. Smith	University of Texas, Austin, TX.
John Sonderegger	Montana Bureau of Mines & Geology, Butte, MT.
Neil Stefanides	Union Oil Company, Los Angeles, CA.
R.C. Stoker	EG&G Idaho, Idaho Falls, ID.
Reid Stone	USGS, Menlo Park, CA.
Paul V. Storm	California Energy Company, Santa Rosa, CA.
W.K. Summers	W.K. Summers & Associates, Socorro, NM.
Chandler Swanberg	New Mexico State University, Las Cruces, NM.
Charles M. Swift, Jr.	Chevron Oil Company, San Francisco, CA.
J.B. Syptak	Anadarko Production Company, Houston, TX.
Robert L. Tabbert	Atlantic Richfield Company, Dallas, TX.
Bernard Tillement	Aquitaine Company of Canada, Calgary, Canada.
Ronald Toms	DOE/DGE, Washington, DC.
Dennis T. Trexler	Nevada Bureau of Mines & Geology, Reno, NV.
John Tsiaperas	Shell Oil Company, Houston, TX.
Jack Von Hoene	Davon, Inc., Milford, UT.
John Walker	DOE/DGE, Washington, DC.
D. Roger Wall	Aminoil USA, Inc., Santa Rosa, CA.

Paul Walton
Maggie Widmayer
Syd Willard
David Williams
Paul Witherspoon
Harold Wollenberg
William B. Wray, Jr.

B.J. Wynat
Paul C. Yuen
S.H. Yungul
Eliot J. Zais

American Geological Enterprises, Inc., Salt
Lake City, UT.
DOE/ID, Idaho Falls, ID.
California Energy Commission, Sacramento, CA.
DOE/DGE, Washington, DC.
Lawrence Berkeley Laboratory, Berkeley, CA.
Lawrence Berkeley Laboratory, Berkeley, CA.
VanCott, Bagley, Cornwall & McCarthy, Salt Lake
City, UT.
Occidental Geothermal, Inc., Bakersfield, CA.
University of Hawaii @ Manoa, Honolulu, HI.
Chevron Resources Company, San Francisco, CA.
Elliot Zais & Associates, Corvallis, OR.

Internal

W. Ursenbach
S.H. Ward (2)
J.A. Whelan
P.M. Wright
H.P. Ross
R.C. Fox
Master Report File

UURI, Salt Lake City, UT.
UU/GG, Salt Lake City, UT.
UU/GG, Salt Lake City, UT.
ESL/UURI, Salt Lake City, UT.
ESL/UURI, Salt Lake City, UT.
ESL/UURI, Salt Lake City, UT.
ESL/UURI, Salt Lake City, UT.

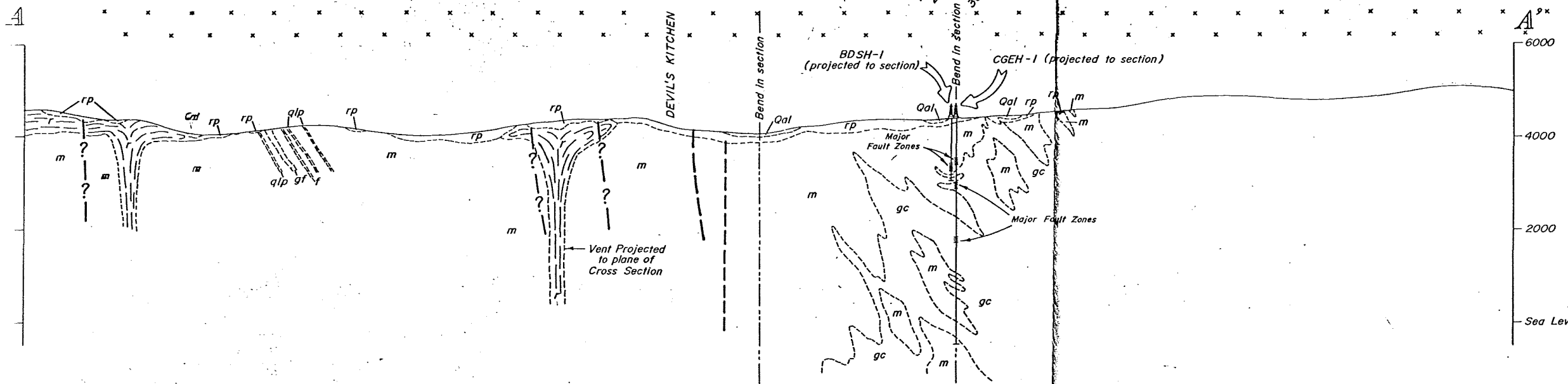
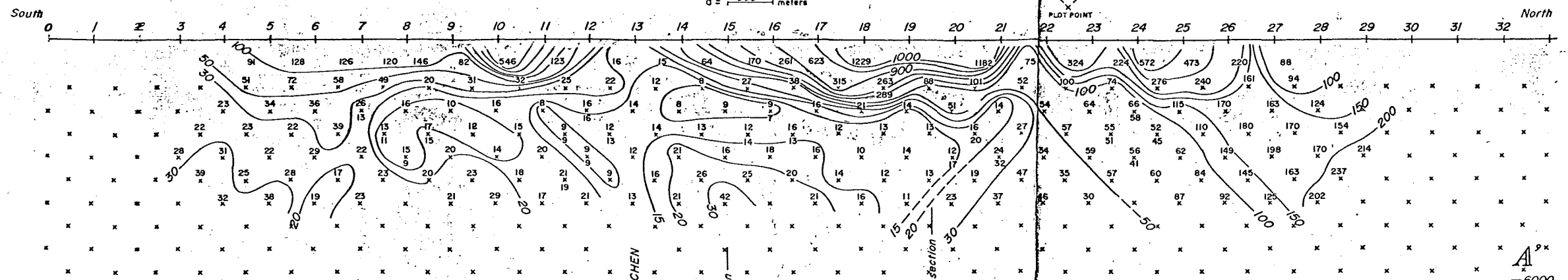
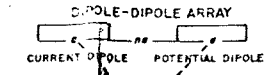
GLO3110-A

EARTH SCIENCE LABORATORY
UNIVERSITY of UTAH RESEARCH INSTITUTE

FIGURE 5

DIPOLE - DIPOLE ARRAY APPARENT RESISTIVITY

$a = 300$ meters

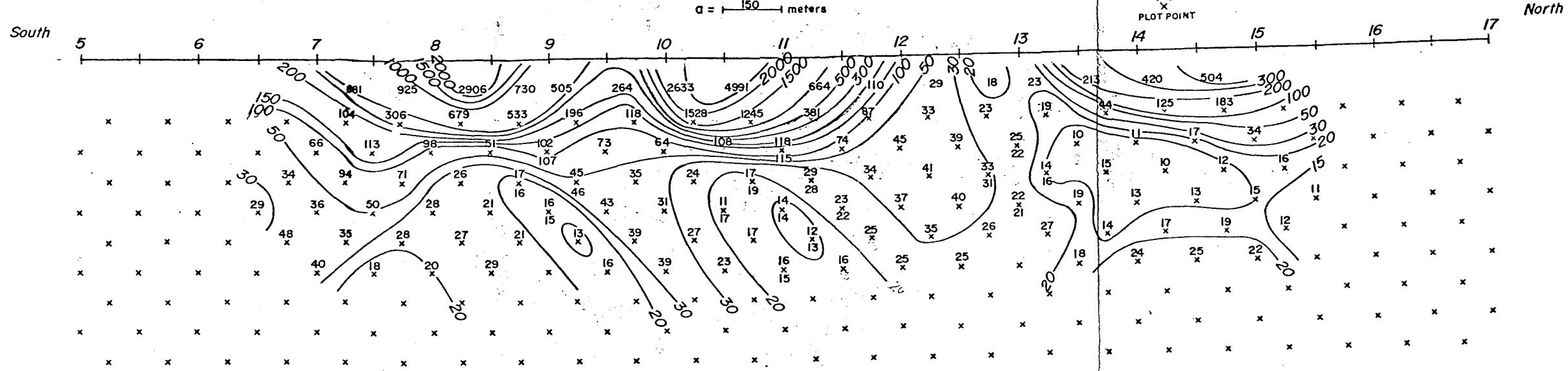
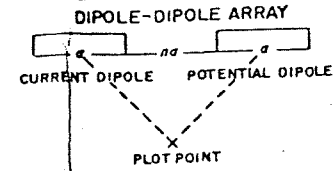


AREA COSO HOT SPRINGS STATE CALIFORNIA LINE 2 DATA BY RCF DATE 9-10-77 TRANSMITTER FT 20 A RECEIVER NEWMONT TYPE

EARTH SCIENCE LABORATORY
UNIVERSITY of UTAH RESEARCH INSTITUTE

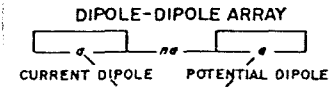
DIPOLE - DIPOLE ARRAY
APPARENT RESISTIVITY

$a = 150$ meters

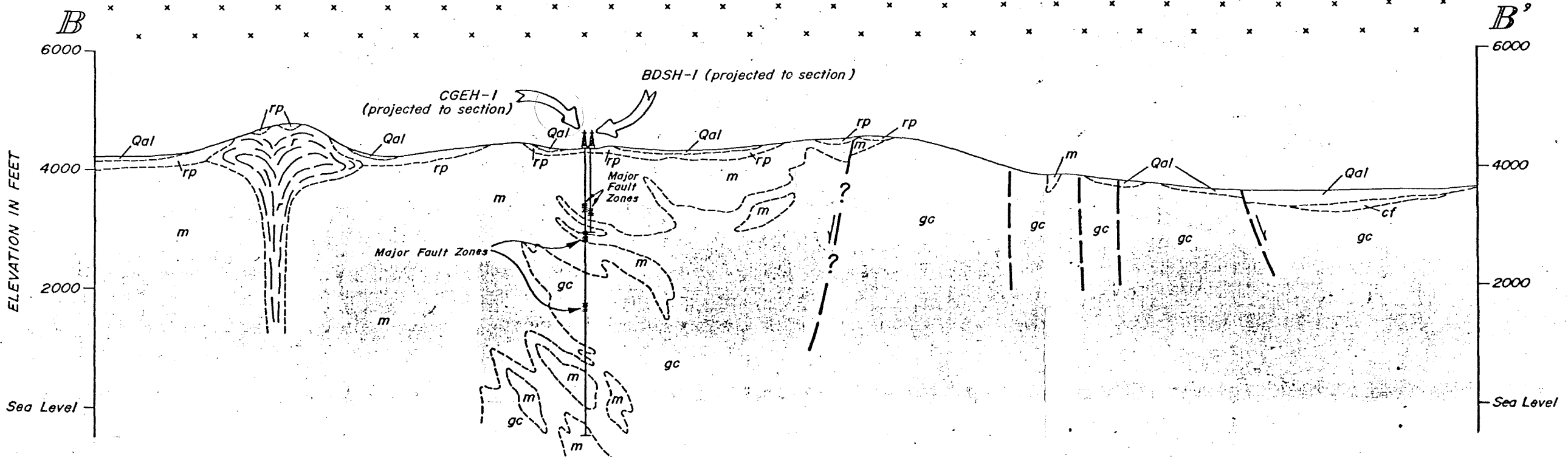
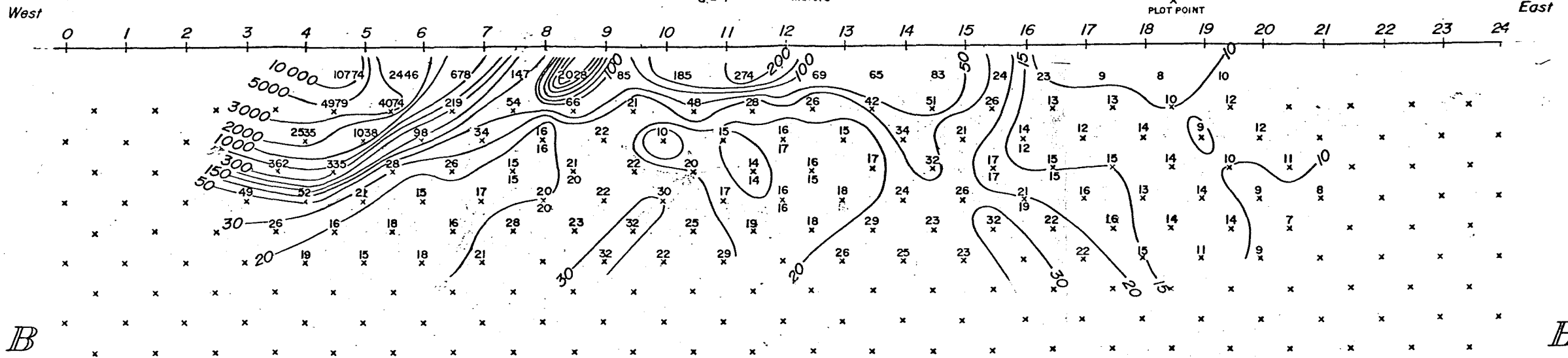


EARTH SCIENCE LABORATORY
UNIVERSITY of UTAH RESEARCH INSTITUTE

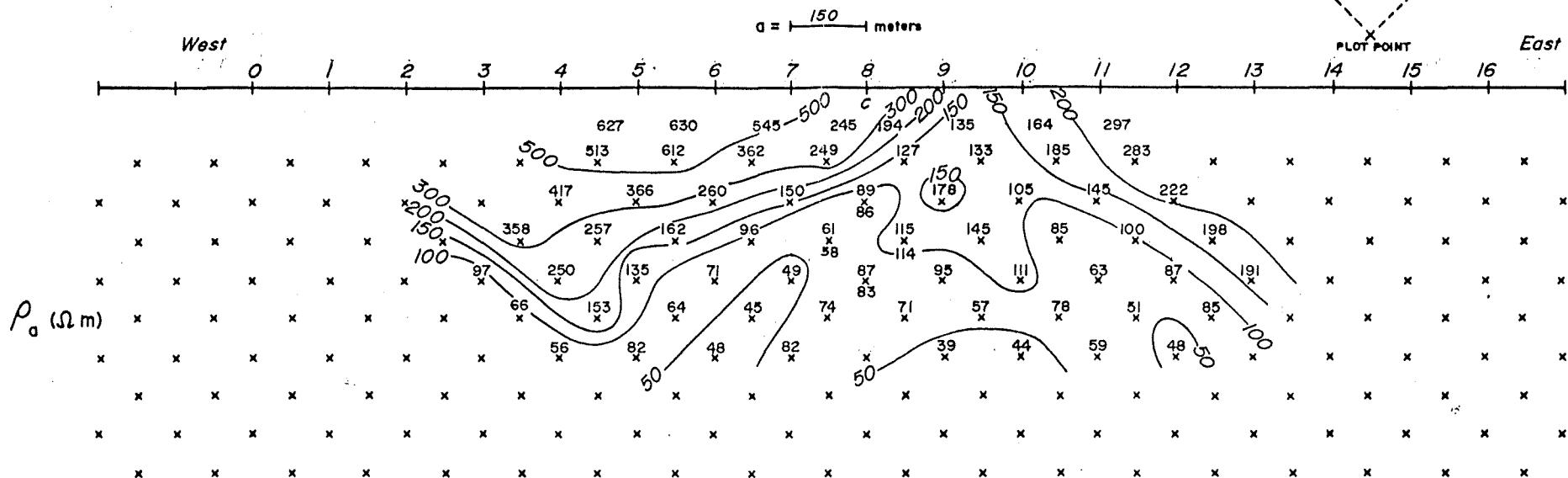
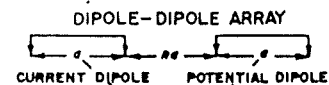
DIPOLE - DIPOLE ARRAY
APPARENT RESISTIVITY



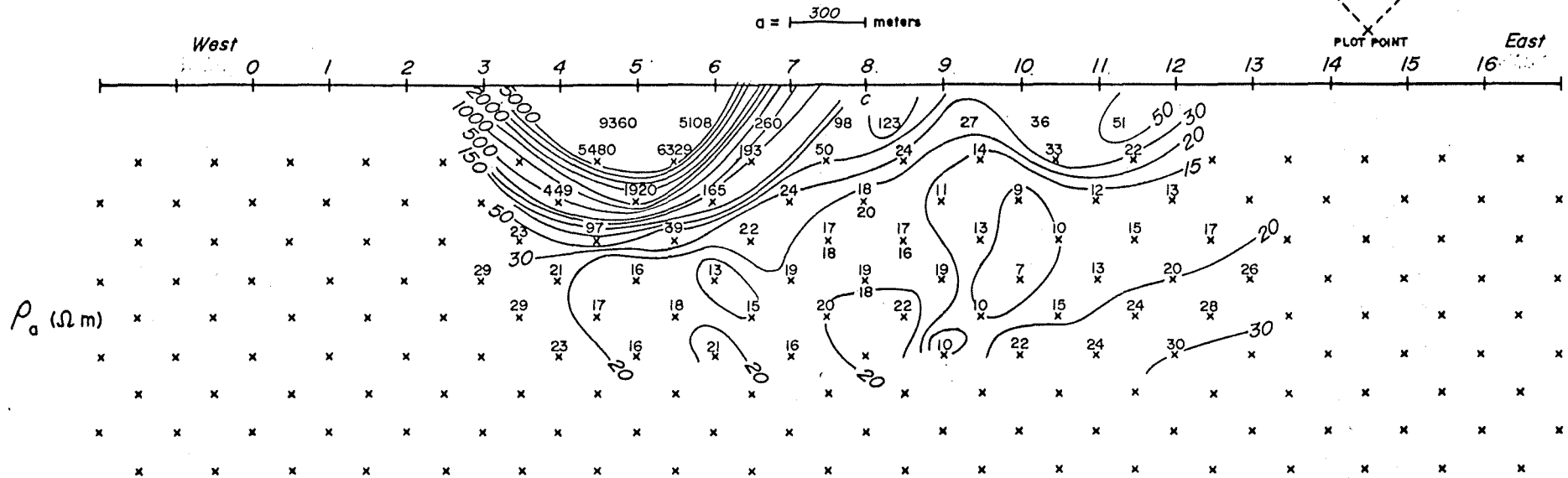
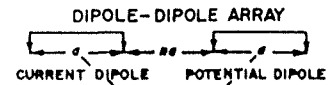
$a = 300$ meters



DIPOLE - DIPOLE ARRAY
 APPARENT RESISTIVITY



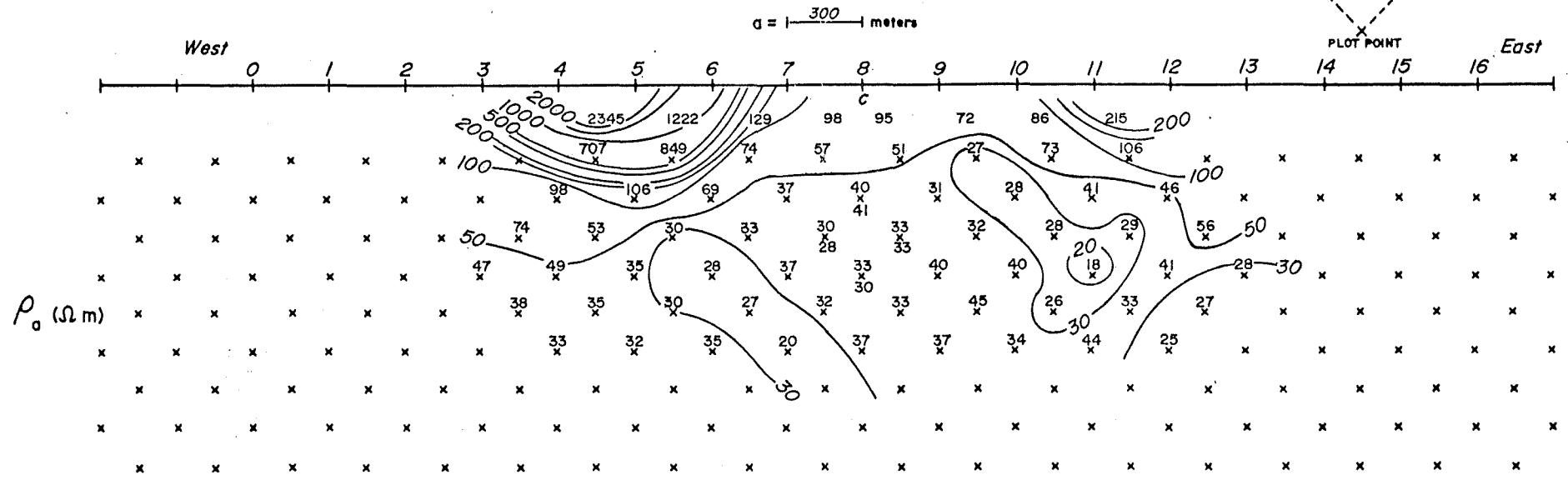
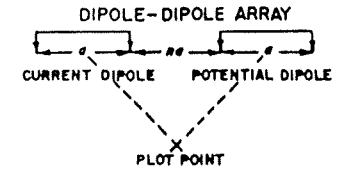
DIPOLE - DIPOLE ARRAY
 APPARENT RESISTIVITY



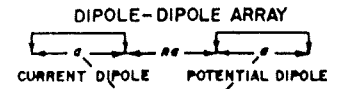
EARTH SCIENCE LABORATORY
UNIVERSITY of UTAH RESEARCH INSTITUTE

FIGURE 10

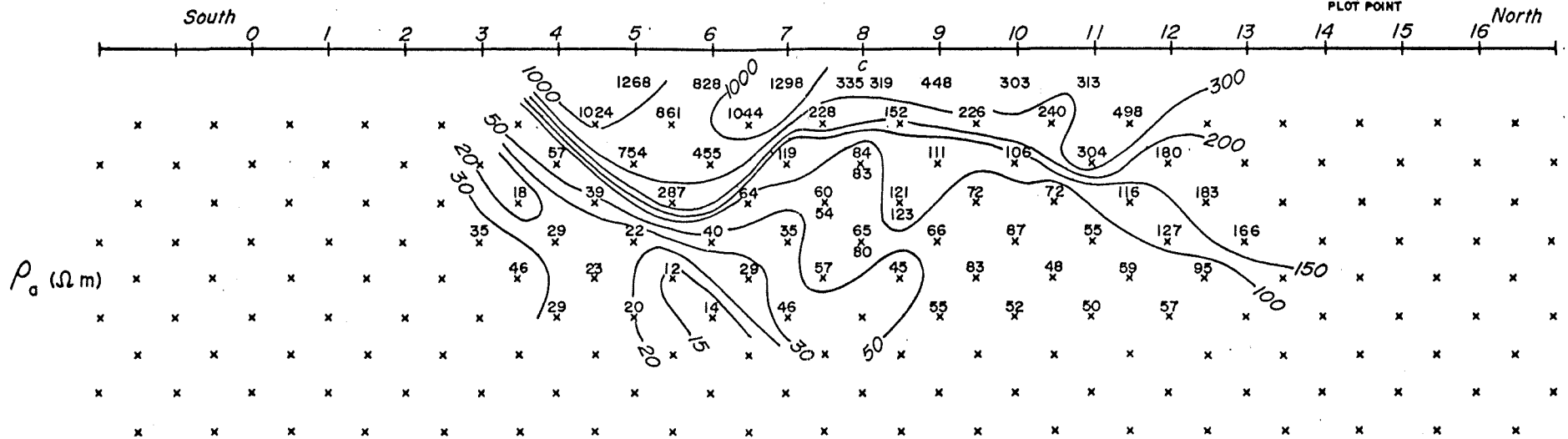
DIPOLE - DIPOLE ARRAY
APPARENT RESISTIVITY



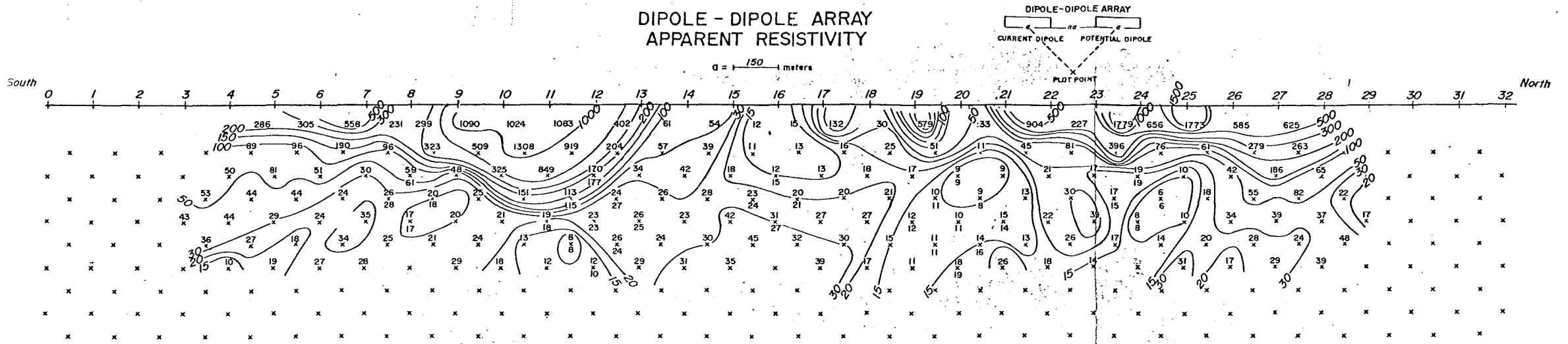
DIPOLE - DIPOLE ARRAY
APPARENT RESISTIVITY



$a = 300$ meters



DIPOLE - DIPOLE ARRAY
APPARENT RESISTIVITY

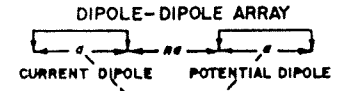


AREA COSO HOT SPRINGS STATE CALIFORNIA LINE 8 DATA BY RCF DATE 9-23-77 TRANSMITTER FT-20A RECEIVER NEWMONTTYPE

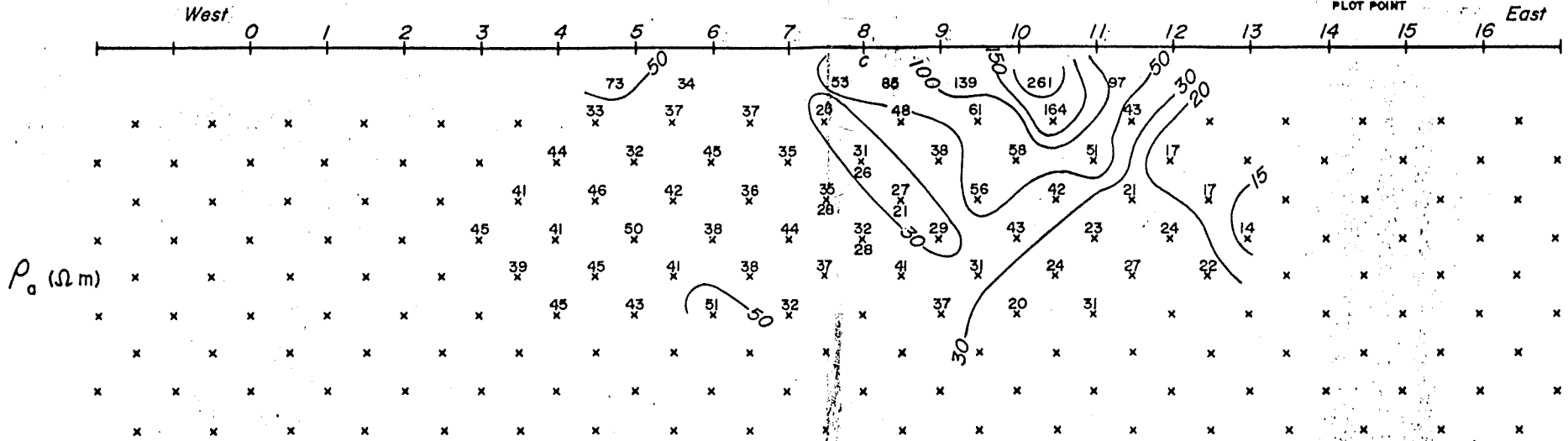
EARTH SCIENCE LABORATORY
 UNIVERSITY of UTAH RESEARCH INSTITUTE

FIGURE 13

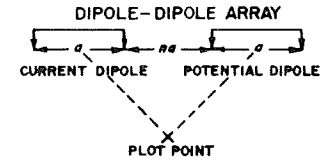
DIPOLE - DIPOLE ARRAY
 APPARENT RESISTIVITY



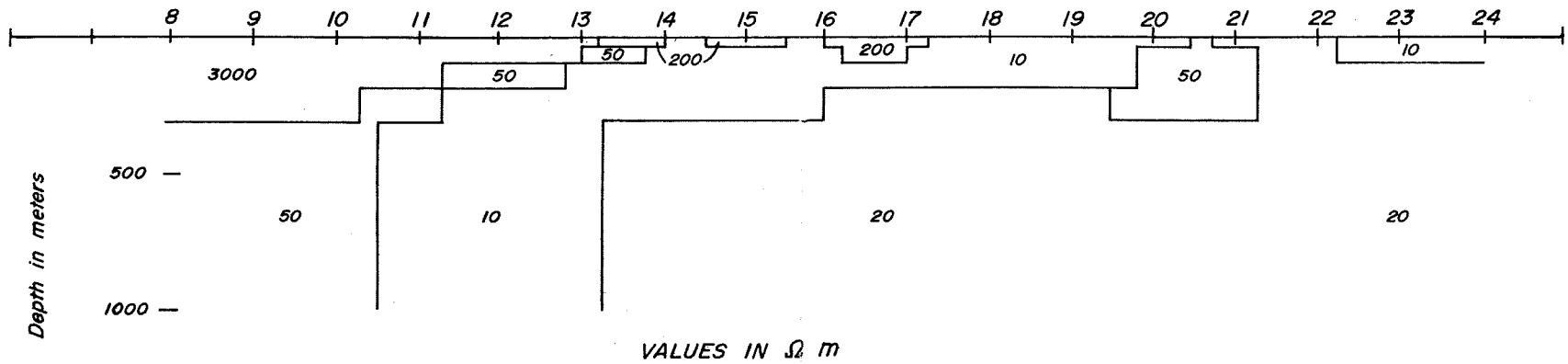
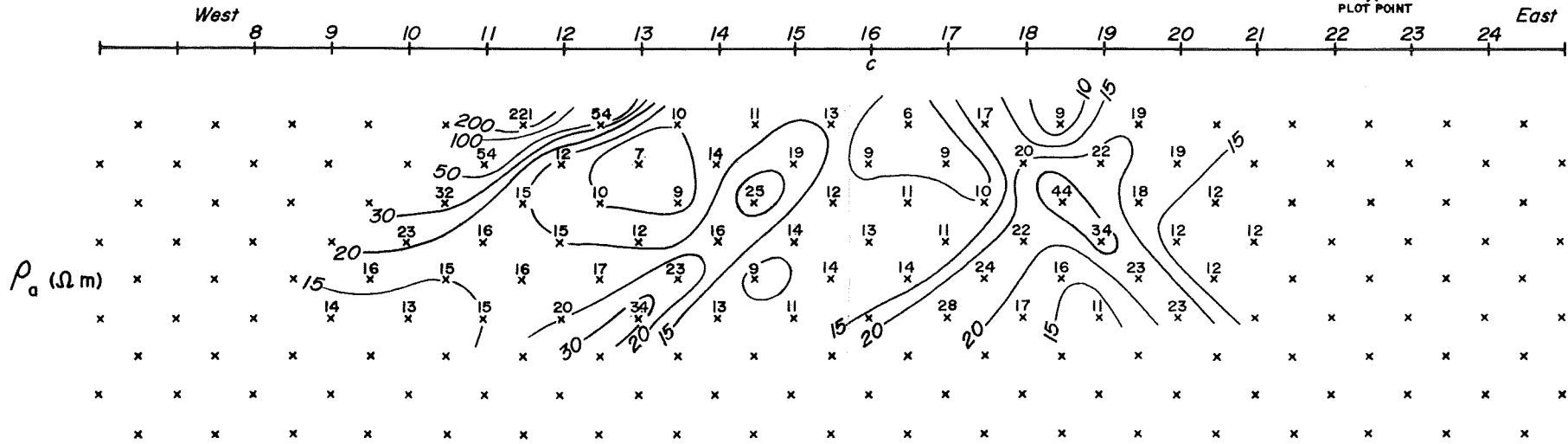
$a = 150$ meters



DIPOLE - DIPOLE ARRAY
APPARENT RESISTIVITY

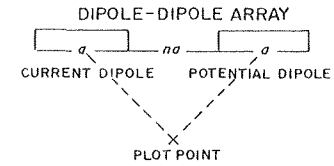


$a = 300$ meters



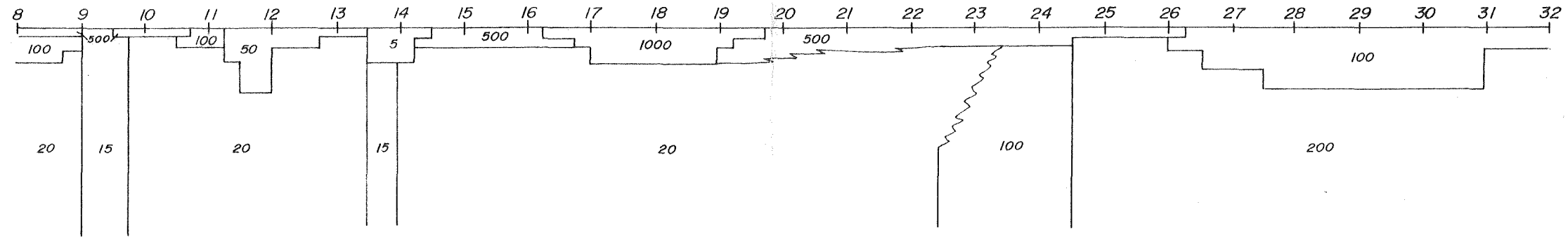
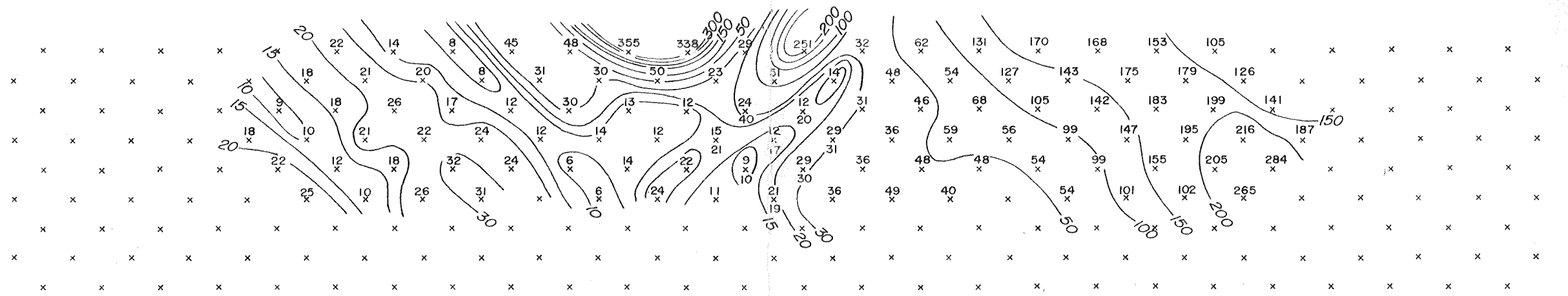
COMPUTER MODEL for LINE 1
Station 8 through Station 24

DIPOLE - DIPOLE ARRAY
APPARENT RESISTIVITY



$a = 300$ meters

South 8 9 10 11 12 13 14 15 16 17 18 19 20 21 22 23 24 25 26 27 28 29 30 31 32 North

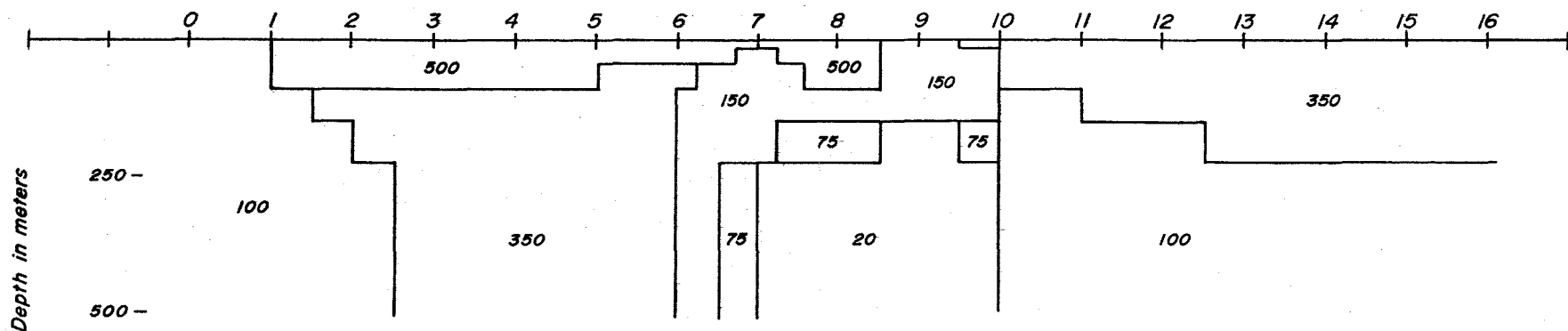
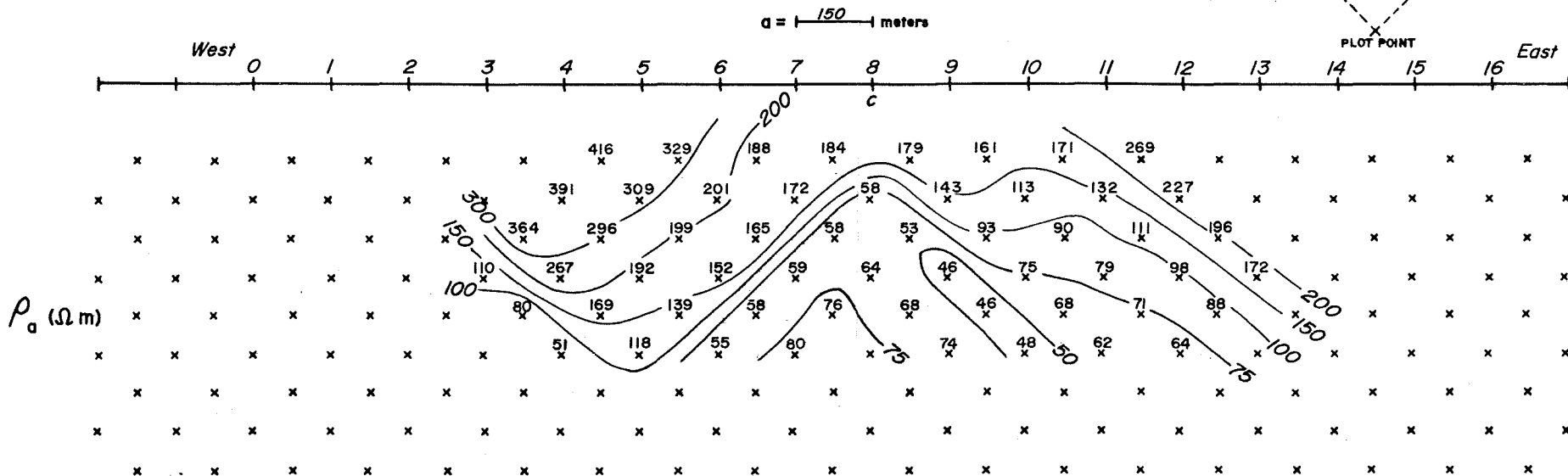
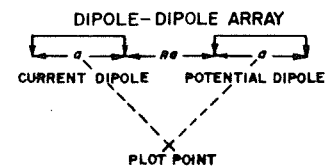


VALUES IN Ωm

COMPUTER MODEL for LINE 2 (300 m)
Station 8 through Station 32

Depth in meters

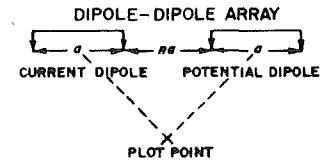
DIPOLE - DIPOLE ARRAY
APPARENT RESISTIVITY



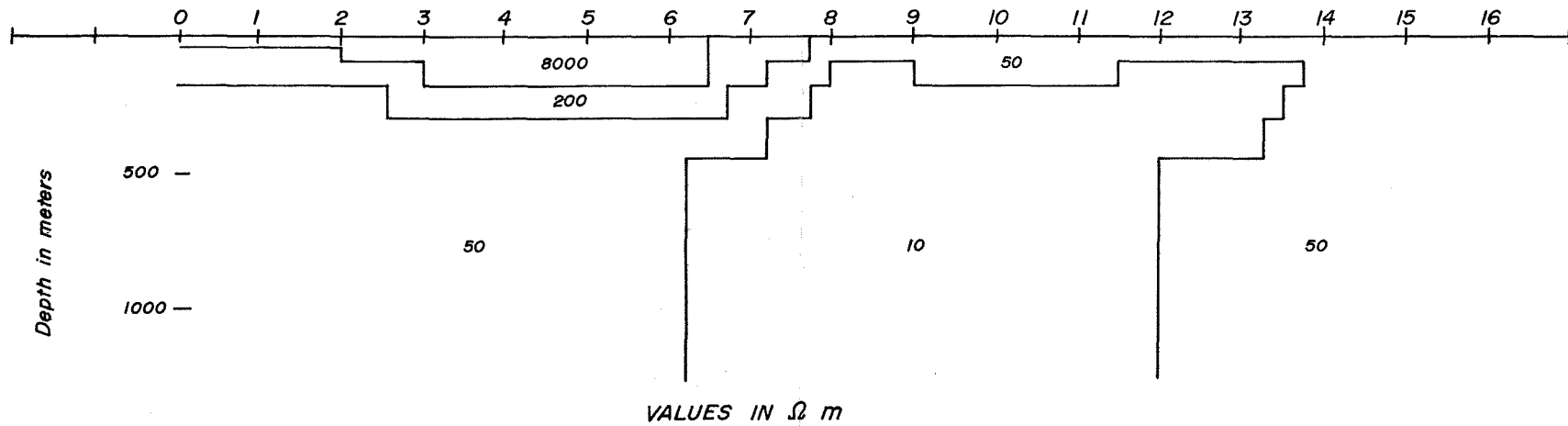
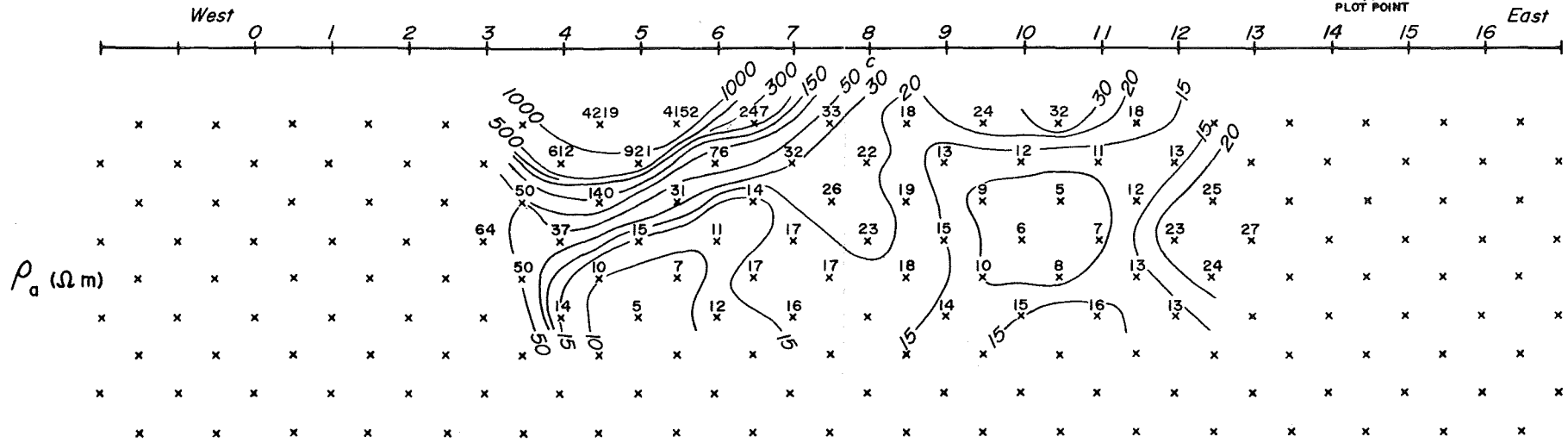
VALUES IN Ωm

COMPUTER MODEL for LINE 4

DIPOLE - DIPOLE ARRAY
APPARENT RESISTIVITY



$a = 300$ meters

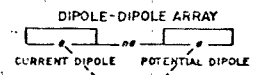


COMPUTER MODEL for LINE 5

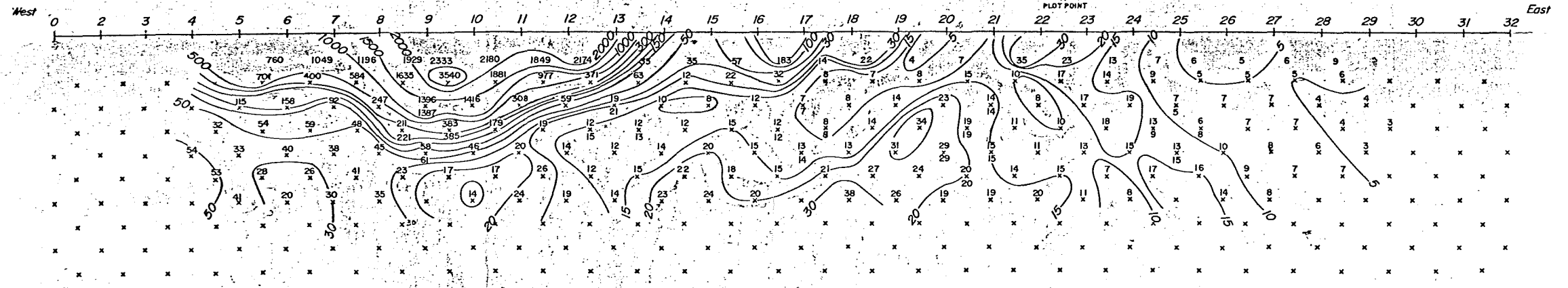
FIGURE 4

EARTH SCIENCE LABORATORY
UNIVERSITY of UTAH RESEARCH INSTITUTE

DIPOLE - DIPOLE ARRAY
APPARENT RESISTIVITY



0 = 300 meters



AREA COSO HOT SPRINGS STATE CALIFORNIA LINE 1 DATA BY RCF DATE 9-9-77 TRANSMITTER FT-20A RECEIVER NEWMONT TYPE